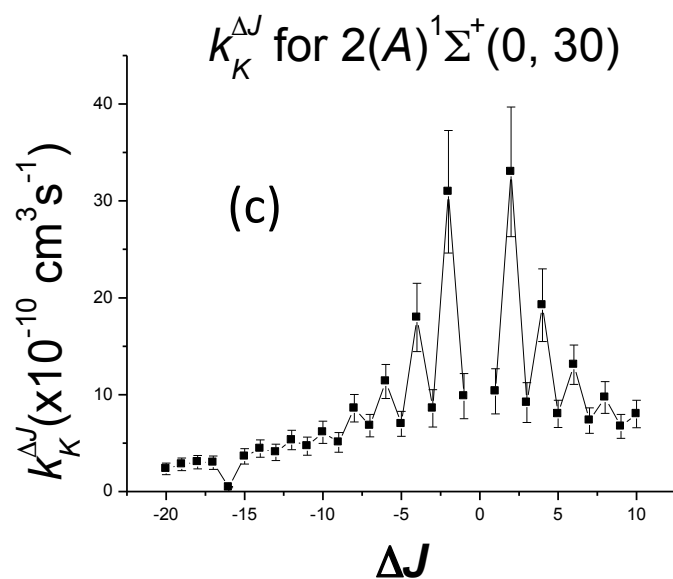
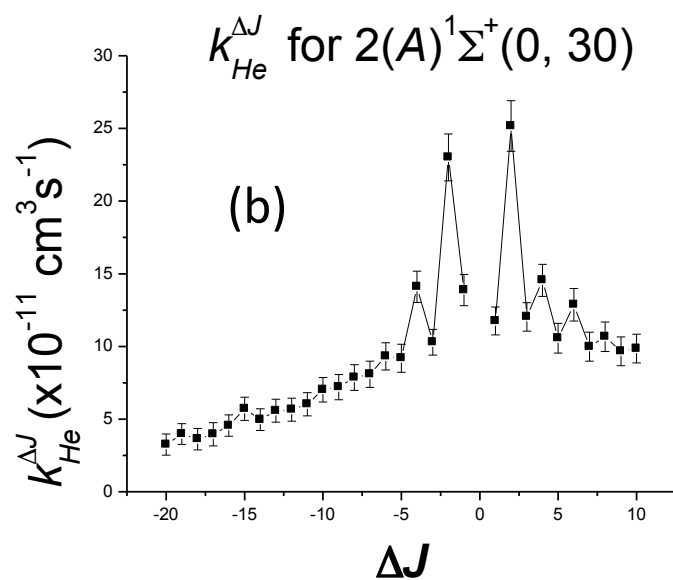
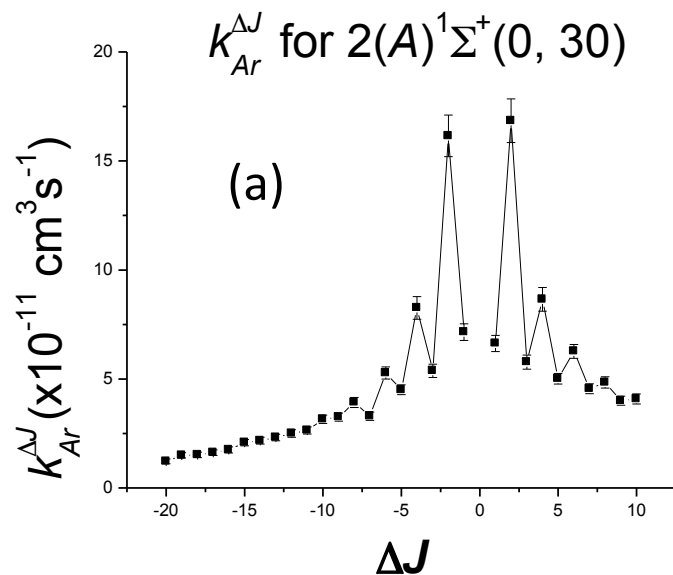
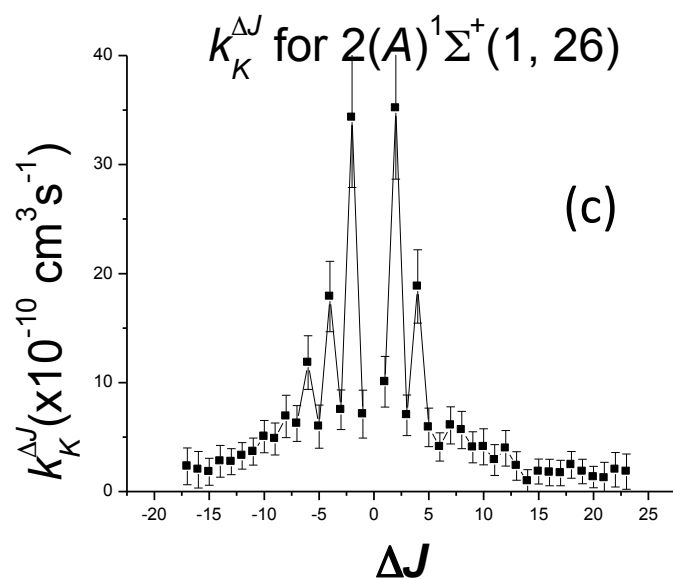
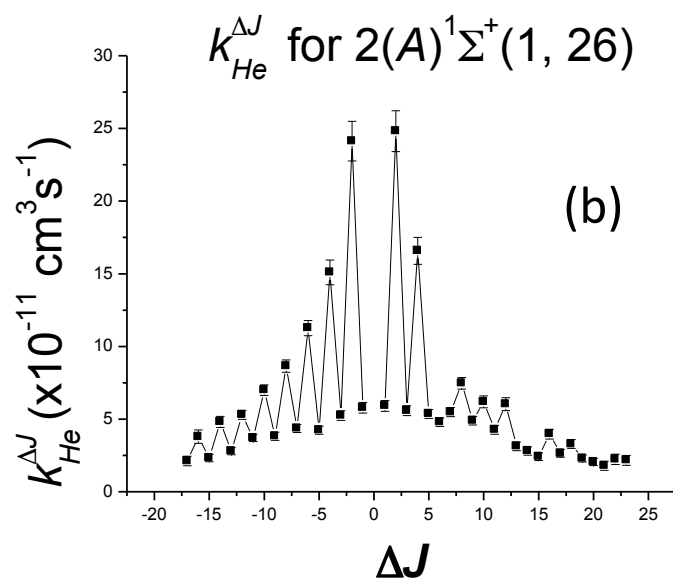
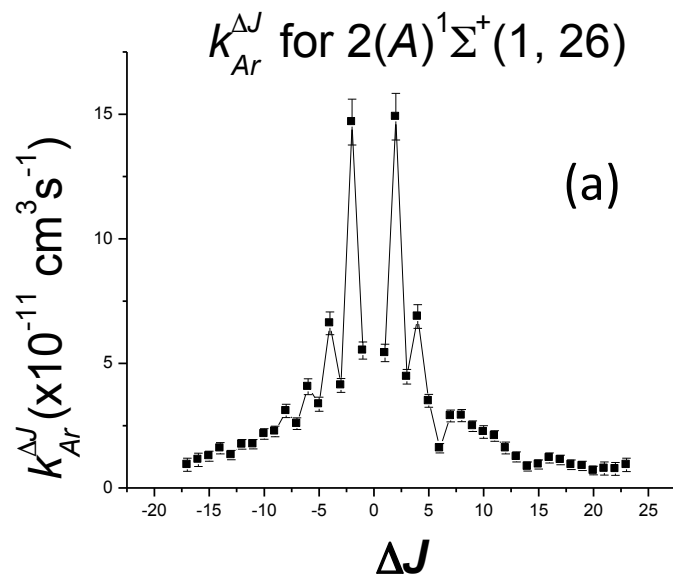


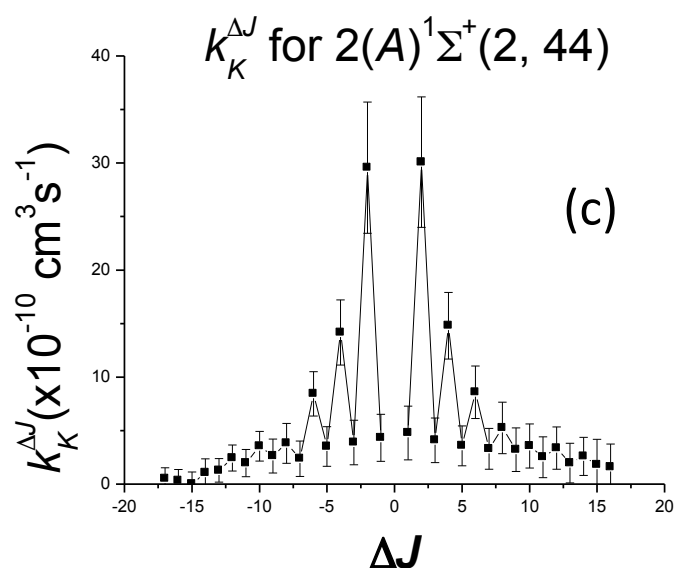
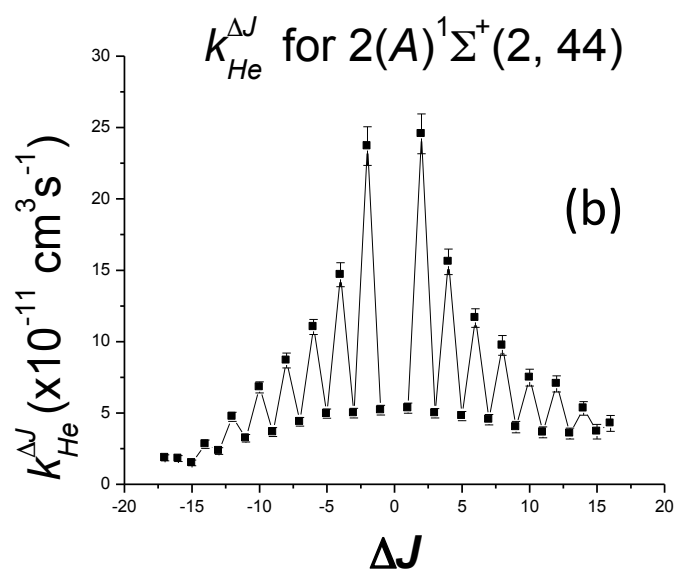
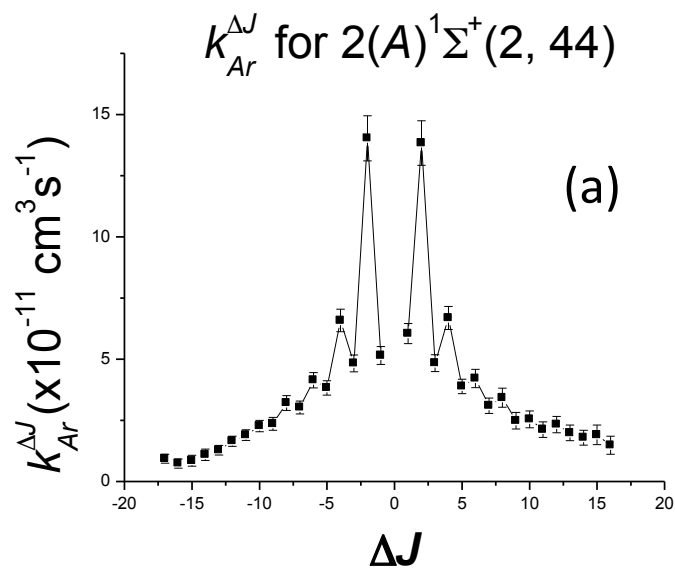
Supplementary Material Fig. 27: Rate coefficients for rotationally inelastic collisions of NaK $2(A)^1\Sigma^+(v=0, J=14)$ molecules with (a) argon, (b) helium, and (c) potassium atoms as functions of ΔJ .



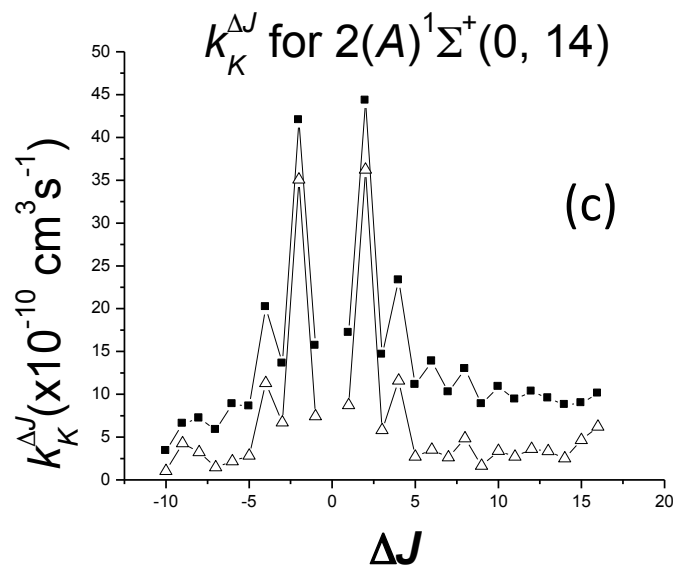
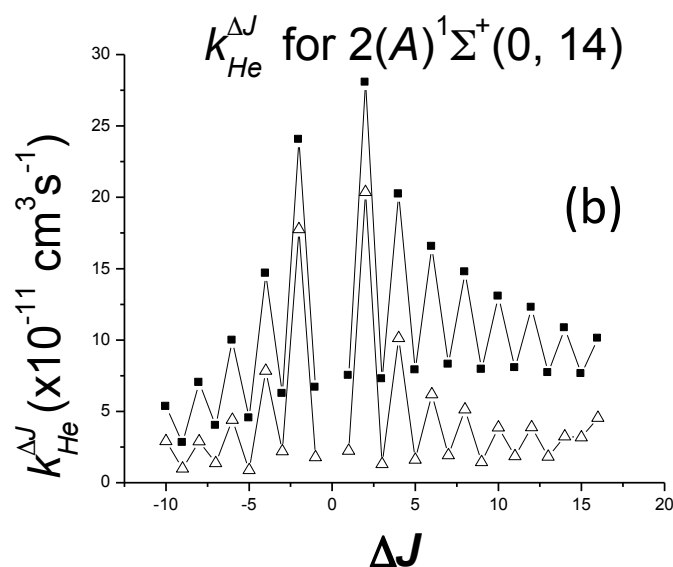
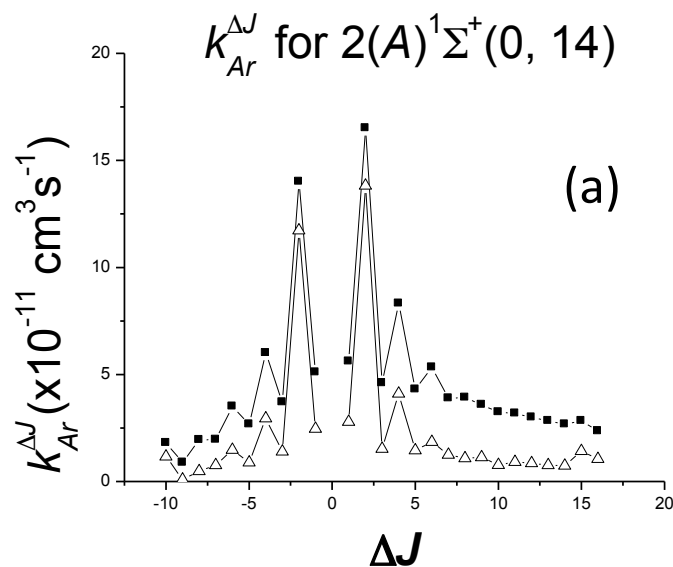
Supplementary Material Fig. 28: Rate coefficients for rotationally inelastic collisions of NaK $2(A)^1\Sigma^+(v=0, J=30)$ molecules with (a) argon, (b) helium, and (c) potassium atoms as functions of ΔJ .



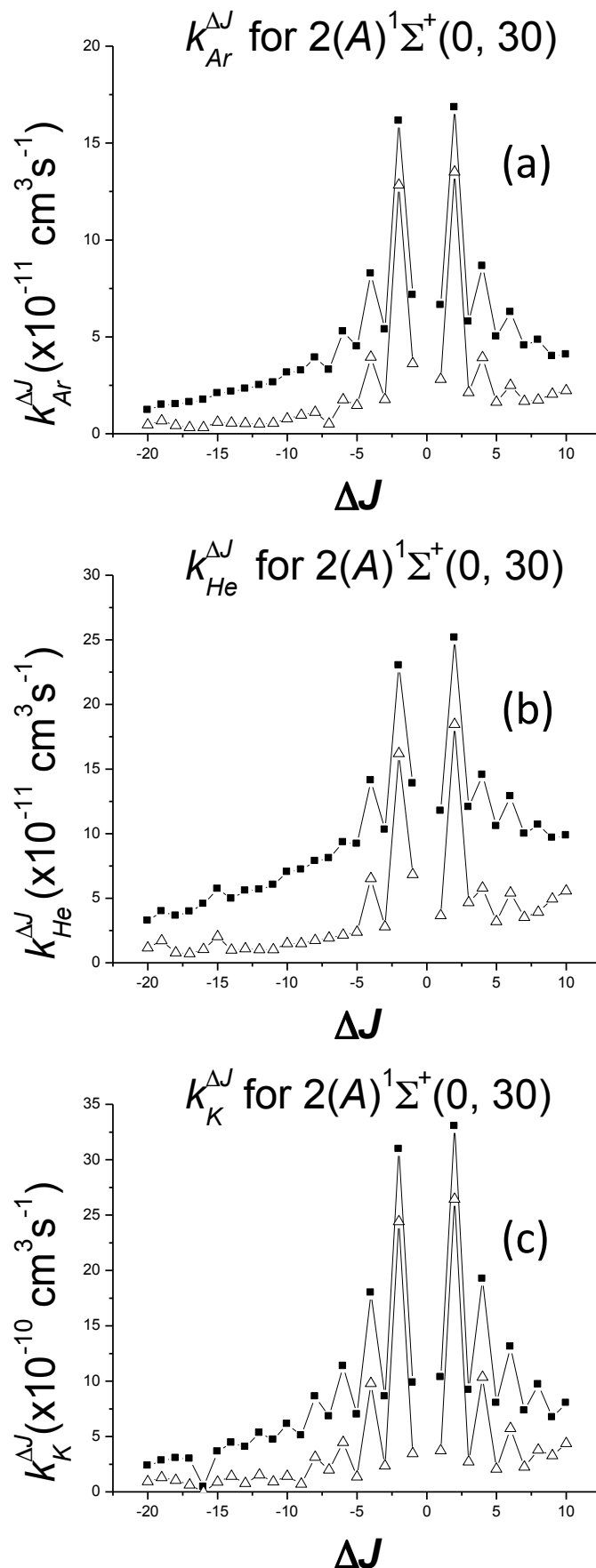
Supplementary Material Fig. 29: Rate coefficients for rotationally inelastic collisions of NaK $2(A)^1\Sigma^+(v=1, J=26)$ molecules with (a) argon, (b) helium, and (c) potassium atoms as functions of ΔJ .



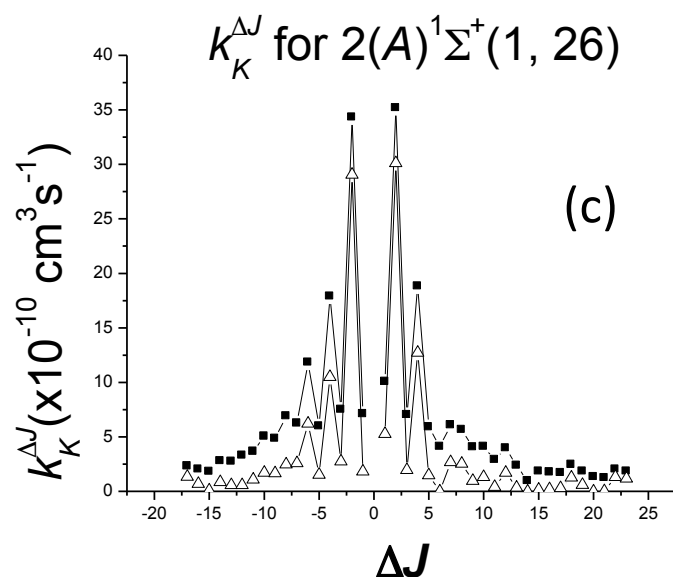
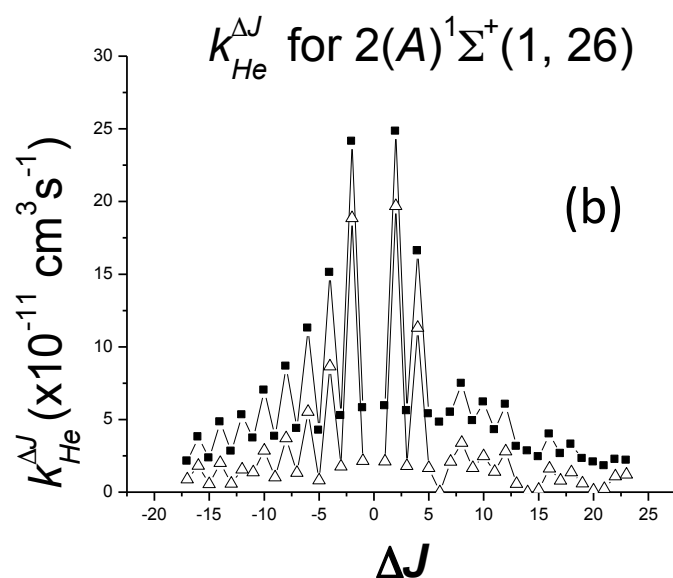
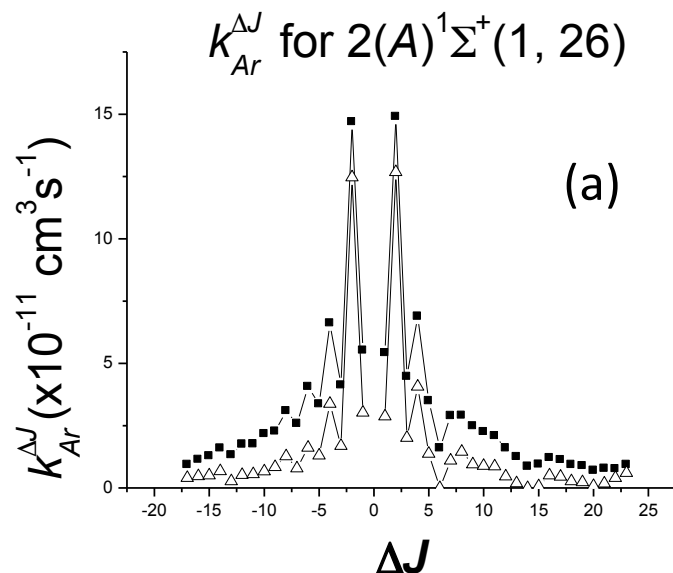
Supplementary Material Fig. 30: Rate coefficients for rotationally inelastic collisions of NaK $2(A)^1\Sigma^+(v=2, J=44)$ molecules with (a) argon, (b) helium, and (c) potassium atoms as functions of ΔJ .



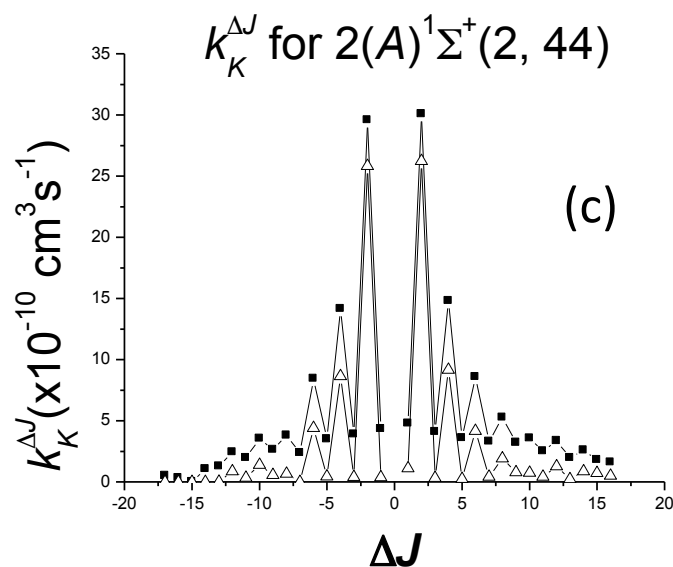
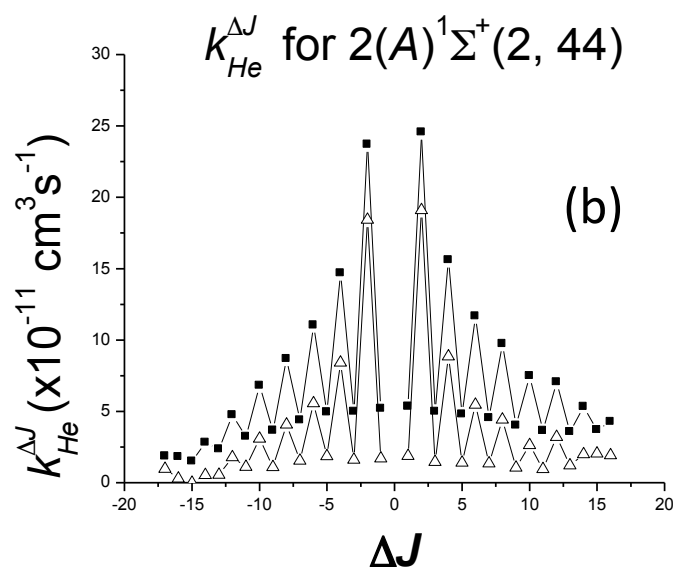
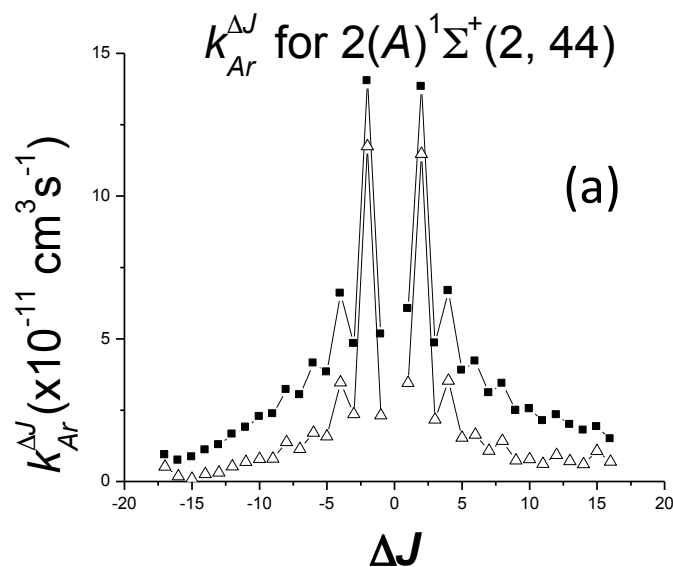
Supplementary Material Fig. 31: Comparison of zeroth order (fit neglecting multiple collision effects – solid symbols) and final rate coefficients including multiple collision effects (open symbols) for rotationally inelastic collisions of NaK $2(A)^1\Sigma^+(v=0, J=14)$ molecules with (a) argon, (b) helium, and (c) potassium atoms as functions of ΔJ . The final values were obtained from the average of the 99th and 100th iterations for (a) and (c) and from the average of the 5th and 6th iterations for (b).



Supplementary Material Fig. 32: Comparison of zeroth order (fit neglecting multiple collision effects – solid symbols) and final rate coefficients including multiple collision effects (open symbols) for rotationally inelastic collisions of NaK $2(A)^1\Sigma^+(v=0, J=30)$ molecules with (a) argon, (b) helium, and (c) potassium atoms as functions of ΔJ . The final values were obtained from the average of the 5th and 6th iterations for (a), (b), and (c).



Supplementary Material Fig. 33: Comparison of zeroth order (fit neglecting multiple collision effects – solid symbols) and final rate coefficients including multiple collision effects (open symbols) for rotationally inelastic collisions of NaK $2(A)^1\Sigma^+(v=1, J=26)$ molecules with (a) argon, (b) helium, and (c) potassium atoms as functions of ΔJ . The final values were obtained from the average of the 99th and 100th iterations for (a) and (c) and from the average of the 5th and 6th iterations for (b).



Supplementary Material Fig. 34: Comparison of zeroth order (fit neglecting multiple collision effects – solid symbols) and final rate coefficients including multiple collision effects (open symbols) for rotationally inelastic collisions of NaK $2(A)^1\Sigma^+(v=2, J=44)$ molecules with (a) argon, (b) helium, and (c) potassium atoms as functions of ΔJ . The final values were obtained from the average of the 99th and 100th iterations for (a) and (c) and from the average of the 999th and 1000th iterations for (b).